Organic & Biomolecular Chemistry

Dynamic Article Links

Cite this: *Org. Biomol. Chem.*, 2011, **9**, 7448

www.rsc.org/obc

PAPER

Multivalent interaction and selectivities in selectin binding of functionalized gold colloids decorated with carbohydrate mimetics†

Meike Roskamp,[a] Sven Enders,[b] Fabian Pfrengle,[a] Shahla Yekta,[a] Vjekoslav Dekaris,[a] Jens Dernedde,[b] Hans-Ulrich Reissig[a] and Sabine Schlecht*‡[a]

Received 12th April 2011, Accepted 26th May 2011
DOI: 10.1039/c1ob05583f

Colloidal gold particles with functionalized organic shells were applied as novel selectin binders. The ligand shell was terminated with different monocyclic carbohydrate mimetics as simplified analogs of the sLe^x unit found in biological selectin ligands. The multivalent presentation of the sulfated selectin binding epitopes on the gold particles led to extremely high binding affinities towards L- and P-selectin and IC_{50} values in the subnanomolar range. Depending on the ring size of the sulfated carbohydrate mimetic, its substitution pattern and its configuration, different selectivities for either L-selectin or P-selectin were obtained. These selectivities were not found for gold particles with simple acyclic sulfated alcohols, diols and triols in the ligand shell. In addition, the influence of the particle size and the thickness of the hydrophobic organic shell were systematically investigated.

Introduction

Chronic inflammatory diseases such as arthritis or asthma are accompanied by ongoing extravasation of leukocytes from the blood vessels into the inflammated tissue.[1,2] This involves a multi-step adhesion process initiated by different selectins and their respective carbohydrate ligands on the leukocyte and on the vascular endothelium.[3] As this deregulated efflux of leukocytes contributes to further tissue damage, anti-inflammatory therapy often aims at inhibiting this key step. Among the natural selectin binding ligands the P-selectin binding PSGL-1 (P-selectin glycoprotein ligand-1) has been extensively studied. A crystal structure analysis of the PSGL-1 peptide/P-selectin complex revealed the precise binding of the sialyl Lewis X (sLe^x) unit and of two out of three sulfated tyrosine residues presented on PSGL-1.[4] The PSGL-1 peptide showed a comparable type of interaction with the L-selectin binding pocket.[5] In the course of further investigations of P-selectin binding the tetrasaccharide sLe^x was considered as the minimal binding unit required for high affinity interaction at the glycan binding site. In contrast to binding to P- and L-selectin, where the O-glycan interaction and the binding of sulfated tyrosin moieties is involved, the interaction of PSGL-1 with E-selectin is achieved by the glycan binding alone and does not involve any sulfate units.[6] Following the investigations of natural ligands of the selectins, artificial synthetic ligands were sought for in order to establish an anti-inflammatory therapy based on the inhibition of selectin binding. Among the first and most effective selectin binders discovered in this way was heparin, a sulfated glycosaminoglycan.[7,8] Heparin can bind with high affinity to P-selectin and to L-selectin. At first sight this is surprising as heparin does not contain the sLe^x structural motif. The binding interaction is mostly caused by the large number of sulfates presented on the polymeric backbone in a multivalent form. The example of heparin shows two aspects of key significance for the future development of selectin binders in anti-inflammatory therapy: (i) multivalent presentation of binding moieties such as sulfates, (ii) minimization of the saccharide binding units leading to less complex epitopes. The latter is of major importance with respect to the cost and effort entailed by the synthesis of a certain artificial selectin ligand.

Multivalent presentation of binding epitopes is a common concept in ligand–receptor interactions and can result in high affinities of ligands that possess only moderate binding constants in their monovalent form.[9] A relevant synthetic example are gold particles decorated with SDC-1721, a derivative of the HIV fusion inhibitor TAK-779 lacking the ammonium moiety considered necessary for efficient binding. Nonetheless, multivalently presented SDC-1721 on gold nanoparticles can bind as effectively as TAK-779 with the ammonium functionality.[10] A plethora of other useful applications of gold nanoparticles[11,12] and soluble nanostructures in general[13,14] in the life sciences was invented in recent years, many of them exploiting multivalency. Additionally, improved multivalent ligand–receptor interactions in selectin binding were found for multivalently functionalized dendrimers.[15,16]

Following the concept of simplified binding epitopes reducing the synthetic complexity of the molecules immobilized on

[a]*Freie Universität Berlin, Institut für Chemie und Biochemie, Takustr. 3, 14195, Berlin, Germany*
[b]*Charité Universitätsmedizin Berlin, Zentralinstitut für Laboratoriumsmedizin und Pathobiochemie, Hindenburgdamm 30, 12203, Berlin, Germany*

† Electronic supplementary information (ESI) available. See DOI: 10.1039/c1ob05583f

‡ New address: Prof. Dr Sabine Schlecht, Justus-Liebig-Universität Gießen, Institut für Anorganische und Analytische Chemie, Heinrich-Buff-Ring 58, 35392 Gießen, Germany; E-mail: Sabine.Schlecht@anorg.chemie.uni-giessen.de

nanoparticles, we prepared and immobilized a series of monocyclic aminopyrans, aminofurans[17] and acyclic aminopolyols as carbohydrate mimetics. In order to enhance the binding affinities of the resulting gold colloids their hydroxyl groups were converted into sulfate functionalities. The carbohydrate mimetics used here have the advantage of being synthetically well accessible with different substitution patterns and variable configuration. In this way, it was possible to conduct comparative studies of sulfated epitopes of different ring size, polarity, configuration, flexibility and spacer length.

Results and discussion

General aspects and syntheses

Water soluble gold colloids with a terminally functionalized thiol shell were used as scaffolds for the multivalent presentation of binding epitopes (Fig. 1).[18] In different series of experiments the binding epitopes **A** were varied for particles of different size, the influence of the presence or absence of an amide linker **B** was evaluated and the chain length of the alkyl spacer **C** was modified.

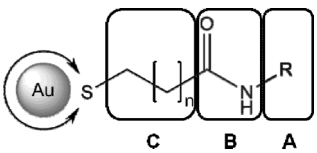

Fig. 1 General schematic representation of the multivalently presented thiols containing a terminal binding epitope **A**, an amide linker **B** (might also be absent) and an alkyl spacer **C**.

Core diameters of the gold colloids of 6 nm and 14 nm were applied in these studies. These colloids can carry, depending on the steric demand of the thiol, between about thousand and five thousand ligands in their shell and therefore provide a high degree of multivalency for the epitope presentation. The smaller functionalized particles were obtained in a highly monodisperse form using a recently published preparation procedure for dodecylthiol (DT) covered colloids[19] and subsequent ligand exchange (Fig. 2). The obtained colloids with a terminal active ester (NHS-ester) group can then be coupled to a primary amine under formation of an amide bond yielding the epitope-containing particles (Fig. 2).

In the case of the larger gold particles with a core diameter of 14 nm a modified citrate-route was used for the synthesis of the particles[20] and the citrate was substituted by the complete

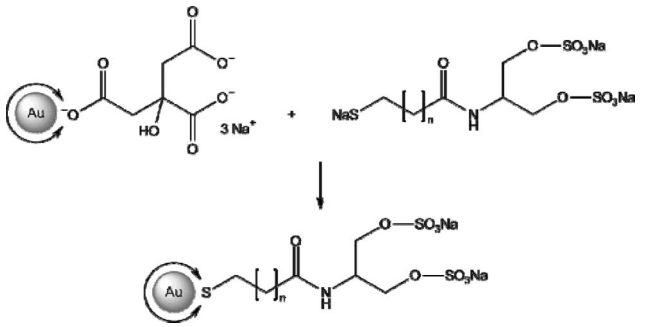

Fig. 3 Preparation of sulfated particles from citrate-stabilized gold colloids (14 nm) and the sodium salt of a sulfated thiolate.

functionalized ligand (mostly already in its sulfated form) that was prepared separately (Fig. 3).

In the case of the smaller colloids where the non-sulfated amino alcohol is coupled to the particle shell, a subsequent sulfation is required. This can be smoothly achieved in anhydrous dimethylformamide (DMF) as a solvent with the DMF-complex of SO_3 (Fig. 4).

Influence of the binding epitope on the selectin binding

The amino alcohols that were immobilized on the particles were varied with respect to their size, their number of hydroxyl groups and their polarity. Monocyclic carbohydrate mimetics in the form of aminopyrans and aminofurans were used as cyclic binding epitopes. Their binding ability was compared to that of acyclic amino alcohols with one, two or three hydroxyl groups. The substitution pattern and the configuration of the aminopyrans and aminofurans were selectively altered in order to present the sulfated hydroxyl groups in variable spatial arrangements and to possibly achieve a selective binding to the different binding pockets of the different selectins. An overview of all amino alcohols that were immobilized on the particle shell is given in Scheme 1.

Our initial experiments with immobilized amino alcohols on the colloids were conducted with the non-sulfated form to probe the validity of the concept of multivalent affinity enhancement of weakly binding or even non-binding epitopes. Therefore the possible binding interaction of aminopyran **1**,[17,21] its N-acylated derivative **1-t** and the functionalized colloid **NP-1** with P-selectin and L-selectin was investigated in a comparative series of measurements in a competitive surface plasmon resonance (SPR) binding assay.[22] Unsubstituted **1** and the derivative **1-t** did not show any inhibition of selectin binding to the assay, neither for P-selectin

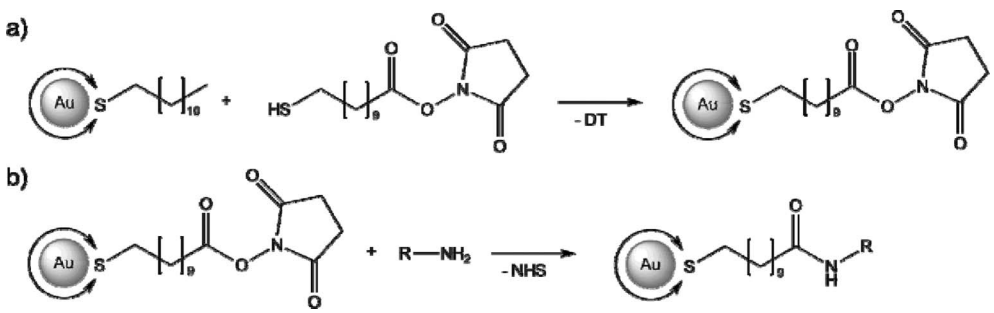

Fig. 2 Ligand exchange (a) and immobilization of amines (b) for the synthesis of terminally functionalized gold colloids (6 nm).

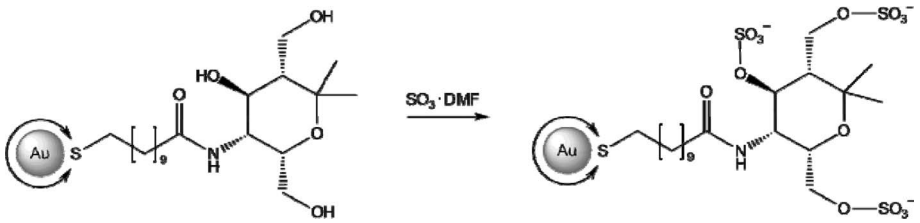

Fig. 4 Synthesis of sulfated colloids (6 nm) containing a carbohydrate mimetic (here compound **1**).

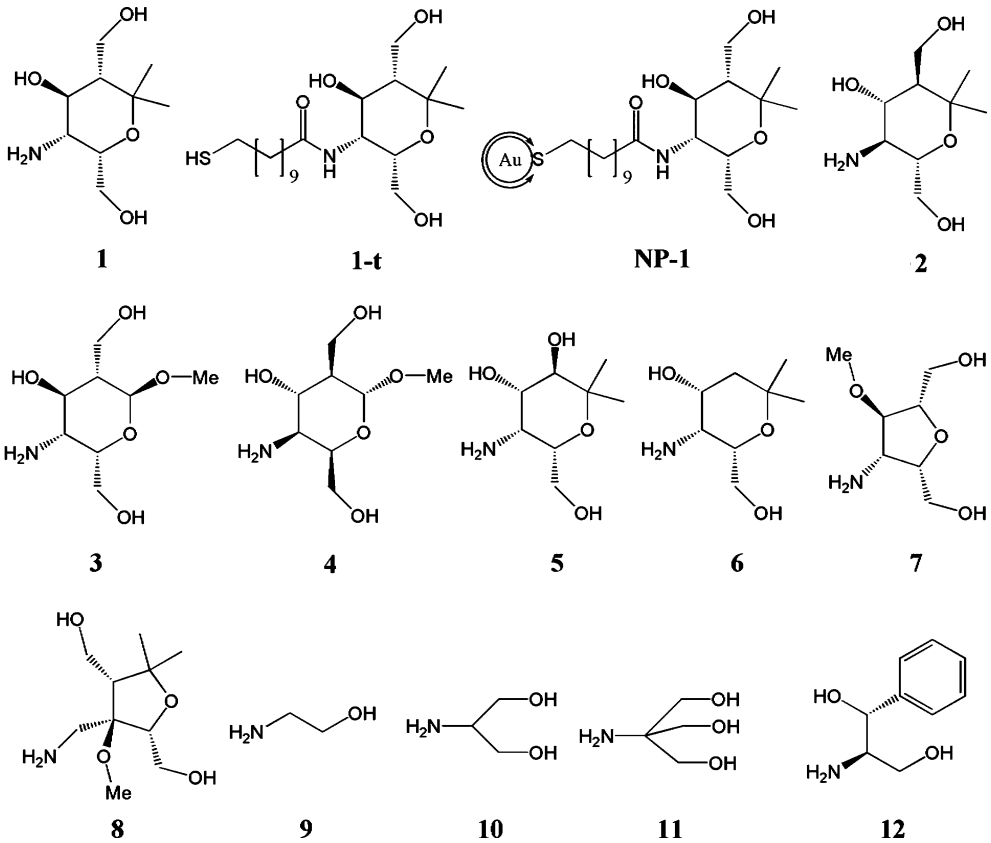

Scheme 1 Aminopyran and aminofuran epitopes and acyclic amino alcohols.

nor for L-selectin (Table 1). In contrast, the 6 nm colloid **NP-1** was found to bind to P-selectin with an IC_{50} value of 10 nM. However, no interaction with L-selectin was detected. The binding of the multivalent colloid of **1** with P-selectin impressively shows the ability of the presentation of a non-interacting molecule on a particle shell to strongly enhance the binding interaction through multivalency. Although **NP-1** can give unambiguous proof-of-principle for the effectiveness of multivalent binding, this colloid is not very suitable for actual medical applications. The colloidal **NP-1** is obtained as a slightly milky solution with limited stability. After a few hours it develops a tendency to flocculate. This is followed by quick precipitation even when the product has been stored in the dark.

Table 1 IC_{50} values for free aminopyran **1**, N-acylated **1-t** and functionalized gold colloid **NP-1**[a]

Inhibitor	IC_{50} (L-selectin)	IC_{50} (P-selectin)
1	n. i.	n. i.
1-t	n. i.	n. i.
NP-1	n. i.	10 nM

[a] n.i.: no inhibition

Because of the limited colloidal stability of **NP-1** and the known improvement of selectin binding for sulfated epitopes we studied the sulfated analogue **NP-1-sulf** for comparison. After sulfation of **NP-1**, the resulting **NP-1-sulf** showed excellent solubility and stability in its colloidal state. The negative charge of the sulfate groups on the stabilizing shell causes interparticle repulsion and a loss of all tendency towards agglomeration. When the selectin binding properties of **NP-1-sulf** were evaluated, binding to L-selectin and P-selectin was found for the sulfated colloid. Both IC_{50} values are lower than that for **NP-1** by several orders of magnitude. For P-selectin a value of 0.04 nM was measured whereas the L-selectin binding revealed an IC_{50} of 0.35 nM (Table 2). In both cases the IC_{50} value was significantly lower than the respective IC_{50} value of heparin of 12 μM for L-selectin. The tendency of **NP-1** to show a stronger interaction with P-selectin is also

Table 2 IC_{50} values for sulfated functionalized gold colloids (6 nm) carrying aminopyran epitopes

inhibitor	IC_{50} (L-selectin)	IC_{50} (P-selectin)
NP-1-sulf	0.35 nM	0.04 nM
NP-2-sulf	0.90 nM	0.20 nM
NP-3-sulf	0.55 nM	0.13 nM
NP-4-sulf	0.60 nM	0.12 nM
NP-5-sulf	0.20 nM	0.46 nM
NP-6-sulf	0.12 nM	0.30 nM

found for its sulfated derivative and this seems to point at a selectivity for the binding pocket of this selectin. The excellent IC_{50} values obtained for **NP-1-sulf** demonstrate that the applied monocyclic carbohydrate mimetic can be a sufficiently complex epitope for very effective selectin interaction. Therefore, we tested a series of other monocyclic amino polyols with five-membered and six-membered rings (Scheme 1) in their sulfated form. Six different aminopyrans and two aminofurans were immobilized on the 6 nm gold colloids, sulfated and evaluated with respect to their selectin binding properties. They all showed IC_{50} values in the sub-nanomolar range and moderate selectivities for either P- or L-selectin (Table 2).

In the case of **NP-1-sulf**, **NP-2-sulf**, **NP-3-sulf** and **NP-4-sulf** the selectivity is in favor of P-selectin, whereas **NP-5-sulf** and **NP-6-sulf** preferentially bind to L-selectin. The applied sulfated aminopyrans differ in their substitution pattern at the six-membered ring, but also in the number of sulfate groups they present to the selectins when bound to the particle. As can be seen from the values of **NP-5-sulf** and **NP-6-sulf** the selectivity is not controlled by the number of sulfates per ring. A replacement of the *gem*-dimethyl substitution at C1 in **1** and **2** by a single methoxy group at this carbon atom in **3** and **4** does not change the selectivity for P-selectin either. Compounds **3** and **4** are enantiomers, but this stereochemical relationship has almost no influence on the IC_{50} values when these two epitopes are connected to the gold colloids and presented in a multivalent fashion. It rather seems to be the relative stereochemical orientation between the amino substituent at C4 used for immobilization and its neighboring sulfates. The aminopyrans **1–4** all have a *trans-trans* configuration of the amino group and the adjacent sulfate substituents at C3 and C2. In contrast, the aminopyrans **5** and **6** do not show this configurational pattern at C2 to C4. After the immobilization and the formation of the amide bond the sulfated heterocycles have to find their best possible conformation for the dense coverage of the colloid surface. The resulting accessibility of the sulfate groups for the different selectins will therefore vary characteristically for different substitution patterns and preferred conformations. The conformation and the orientation of the sulfate groups of **NP-1-sulf** to **NP-4-sulf** is apparently more suitable for binding to P-selectin, whereas the colloids presenting the sulfated aminopyrans **5** and **6** exhibit a stronger interaction with L-selectin.

In addition to the binding studies with colloids carrying sulfated aminopyrans, we also investigated the binding properties of two immobilized and sulfated aminofurans **7** and **8**. Sulfated **7** contains a *trans-trans* substitution pattern similar to aminopyrans **1–4**, whereas the aminofuran **8** does not contain the primary amino group directly at the ring. These structural features lead to slightly better P-selectin binding for **NP-7-sulf** and a moderate L-selectin selectivity for **NP-8-sulf** (Table 3).

Table 3 IC_{50} values for sulfated functionalized gold colloids (6 nm) with aminofurans

Inhibitor	IC_{50} (L-selectin)	IC_{50} (P-selectin)
NP-7-sulf	0.20 nM	0.14 nM
NP-8-sulf	0.15 nM	0.40 nM

Summarizing the binding experiments with functionalized gold colloids presenting sulfated aminopyrans and aminofurans, it can be stated that all particles with carbohydrate mimetic epitopes show excellent potential for an inhibition of the binding of P- and L-selectin to their natural ligands. In all cases IC_{50} values in the sub-nanomolar range were found and the sulfated colloids were stable at least for several months. As these data clearly indicate that the approach using a simplified carbohydrate mimetic epitope presented in a highly multivalent manner on a gold colloid is well suited to obtain high-affinity selectin interactions, we attempted to reduce the immobilized chemical structures even further and functionalized the colloids with simple acyclic aminopolyols. After their attachment to the particle shell they were sulfated like the heterocyclic systems discussed above.

The coupling of amino alcohols with one, two or three hydroxyl groups was achieved by the formation of an amide bond from an NHS ester as described for the cyclic analogues. Complete sulfation of the product colloids was again obtained by reaction with SO_3·DMF. The IC_{50} values for binding to P-selectin and L-selectin for a series of four different sulfated colloids were measured (Table 4).

The functionalized gold colloids with acyclic epitopes also show excellent binding to both selectins in the sub-nanomolar range, in some cases with even lower IC_{50} values than the cyclic compounds. But in contrast to the sulfated aminopyrans and aminofurans all acyclic epitopes exhibited no significant selectivity in their binding behavior towards the two tested selectins. When the values of the monosulfate **NP-9-sulf**, the disulfate **NP-10-sulf** and the trisulfate **NP-11-sulf** are compared the strongest binding is found for **NP-10-sulf** derived from the aminodiol serinol. For the disulfate the charge density on the surface of the colloid shell and the flexibility of the epitope seem to be ideal for interaction with the binding pocket. Colloids covered with a monosulfate bind more weakly, most likely because of the smaller number of sulfate groups available in their shell. Unlike the disulfate case, the trisulfated amino alcohol does not improve the IC_{50} values. A possible reason might be the high steric demand of the trisulfate, reducing the packing density of the ligand shell and creating more steric hindrance in the binding pocket. When the phenyl-substituted **NP-12-sulf** was investigated in order to check the influence of the bulky apolar substituent, an even bigger negative impact on

Table 4 IC_{50} values for sulfated functionalized gold colloids (6 nm) carrying different acyclic epitopes

Inhibitor	IC_{50} (L-selectin)	IC_{50} (P-selectin)
NP-9-sulf	0.18 nM	0.22 nM
NP-10-sulf	0.02 nM	0.03 nM
NP-11-sulf	0.07 nM	0.09 nM
NP-12-sulf	0.10 nM	0.15 nM

Table 5 IC_{50} values for sulfated functionalized 6 nm and 14 nm gold colloids

Inhibitor	IC_{50} (L-selectin)
NP-9-sulf (6 nm)	0.18 nM
NP-13-sulf (14 nm)	0.13 nM
NP-10-sulf (6 nm)	0.02 nM
NP-14-sulf (14 nm)	0.07 nM
NP-11-sulf (6 nm)	0.07 nM
NP-15-sulf (14 nm)	0.20 nM

the IC_{50} values was detected. Here, the steric hinderance and the hydrophobicity of the phenyl group are both of disadvantage. Although we observe a lack of selectivity in the binding of these acyclic sulfates, the colloid-selectin interaction is strong and there is a tendency for generally lower IC_{50} than for the cyclic analogues.

The consistently good selectin binding properties of the investigated colloids of 6 nm core size asked for an evaluation of similarly functionalized gold particles with a larger core diameter. As already mentioned earlier, these larger particles with functionalized ligand shells (**NP-13-sulf** to **NP-15-sulf**) were obtained by direct ligand exchange from citrate stabilized particles of 14 nm core diameter (Scheme 2, Fig. 3). Only sulfated colloids with acyclic amino alcohols were prepared for this purpose and their values for L-selectin binding were compared with the ones for 6 nm colloids with the same type of functionalized shell (Table 5).

The effect of the particle size on the selectin interaction is different for the immobilized monosulfate and for the di- and trisulfates. When the monosulfate is used, the bigger particle size leads to a slightly improved selectin interaction, whereas the disulfate and the trisulfate show higher IC_{50} values when the bigger colloids are used. A possible explanation for this phenomenon can be found in the higher packing density of the ligand shell when the curvature is reduced due to the larger particle diameter. The average distance between the terminal binding

Table 6 IC_{50} values for amide-containing **NP-9-sulf** (6 nm) and amide-free **NP-16-sulf** (6 nm)

Inhibitor	IC_{50} (L-selectin)	IC_{50} (*P*-selectin)
NP-9-sulf	0.18 nM	0.22 nM
NP-16-sulf	0.15 nM	0.03 nM

epitopes becomes smaller for larger colloids. This was shown in previous work on particles covered by a dodecylthiol shell[23] and on DNA-functionalized particles.[24] For the bulkier di- and trisulfated systems no further densification of the thiol shell is possible and the reduced curvature of the bigger particles causes a loss of thiols from the particle rather than a denser packing of the shell. As a consequence, the selectin binding is weakened compared with the smaller colloids.

Influence of the amide linker on the selectin binding

As the binding pocket of the respective selectin is prone to polar interaction with the amide bond created in the coupling of the amino alcohol to the particle shell, a comparison of **NP-9-sulf** with **NP-16-sulf** bearing no amide bond reveals significant differences (Table 6). Although the amide bond is not directly solvent-exposed, its presence has a clear impact on the IC_{50} values. The amide-free colloid **NP-16-sulf** shows a similar binding affinity to L-selectin as the amide-containing **NP-9-sulf**, but its IC_{50} value for P-selectin is considerably reduced, thus creating a selectivity between the two selectins that is not observed for any of the amide-coupled acyclic sulfate colloids. It was pointed out in recent work on the interaction of the natural ligand PSGL-1 with P- and L-selectin and the arrangement of the ligand in the binding pockets of these selectins that hydrophobic interactions between leucine and proline residues of PSGL-1 and the selectin play an important role for P-selectin but could not be found for L-selectin binding.[25] Thus,

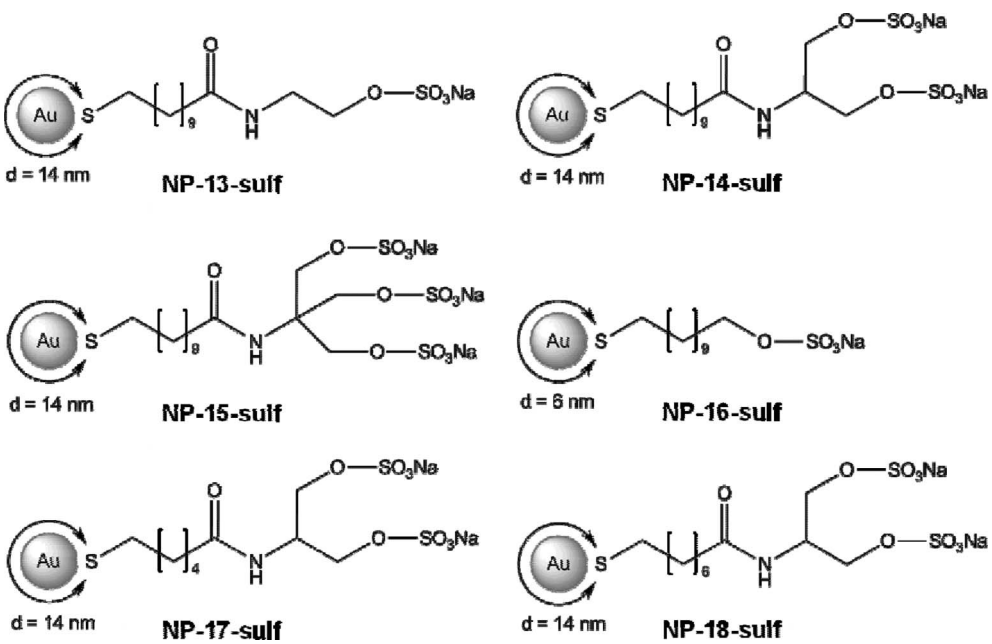

Scheme 2 Functionalized sulfated colloids **NP-13-sulf** to **NP-18-sulf** obtained by direct ligand exchange from Au/dodecanethiol (6 nm) or Au/citrate (14 nm).

the very low IC_{50} value found for P-selectin binding of **NP-16-sulf** can be attributed to a hydrophobic interaction of the alkyl chain within the binding pocket of P-selectin. The presence of the polar amide bond in the thiol shell seems to disturb this interaction and therefore leads to a higher IC_{50} value. It is remarkable that this selectivity is only found for the colloid **NP-16-sulf**. The monovalent sulfated 11-mercapto-undecanol **16-sulf** showed no selectivity and much higher IC_{50} values of 30 μM and 40 μM for L- and P-selectin, respectively. When comparing the IC_{50} values for P-selectin binding of monovalent **16-sulf** and multivalent **NP-16-sulf** it becomes apparent that multivalent presentation of such epitopes on a gold nanoparticle can enhance their biological activity by a factor of up to 10^6.

Influence of the chain length of the alkyl spacer

Aiming at a broader understanding of the parameters involved in the selectin binding of these colloids, we conducted an additional series of experiments varying the chain length of the thiol shell of 14 nm colloids. This will alter the packing density of the epitopes presented on the particle and the degree of the hydrophobic interaction with P-selectin. The thiols used for this study were derived from hexanoic acid, octanoic acid and undecanoic acid (Scheme 2, Table 7). A first tendency found in the data is a stepwise improvement of selectin affinities in variation with the length of the alkyl chain. Both L- and P-selectin prefer colloids with a longer alkyl chain, but the differences in the IC_{50} values between the C6 chain and the C11 chain are much greater for P-selectin. This is not particularly surprising as the hydrophobic interaction that is already weak because of the amide bond is expected to almost disappear for a short chain. Therefore the IC_{50} value for P-selectin found for **NP-17-sulf** is 5.4 times higher than for **NP-14-sulf**, but for L-selectin it is only 2.3 times more. As a consequence, the colloid with the short chain C6 thiol shows a moderate selectivity for L-selectin.

Table 7 IC_{50} values for sulfated functionalized gold colloids (14 nm) with different chain lengths of the spacer molecules of the shell

Inhibitor	IC_{50} (L-selectin)	IC_{50} (P-selectin)
NP-17-sulf	0.16 nM	0.54 nM
NP-18-sulf	0.07 nM	0.13 nM
NP-14-sulf	0.07 nM	0.10 nM

Non-toxicity of the colloids towards Jurkat cells

Given the excellent stability and the very high binding affinity of the sulfated colloids, their possible cytotoxicity towards L-selectin-expressing T-cells was also investigated. All leukocytes constitutively express L-selectin on their cell surface and are therefore targets for the here described functionalized gold colloids. Because of their general importance in immunosurveillance we chose a T-cell line (Jurkat) for toxicity studies to show if cellular binding of ligands does interfere with cell proliferation. The three differently functionalized colloids **NP-1-sulf**, **NP-10-sulf** and **NP-16-sulf** were evaluated. Jurkat cells were incubated with colloid solutions in the concentration range from 0.003 nM to 30 nM (Fig. 5). In all cases the cell viability was not reduced. Although the colloids did not show acute toxicity, further analyses are necessary to prove for safety in animal models, also in longitudinal comparative studies. High specifity of gold colloids decorated with carbohydrate mimetics to L- and P-selectin and fast clearance of unbound particles *in vivo* are desirable in order to avoid unwanted side effects. As reviewed recently[29] local and systemic toxicity of nanoparticles is determined by particle composition, dose, size and surface characteristics. In this respect it is noteworthy that citrate-capped gold nanoparticles, even after repeated administration to mice and accumulation in tissues, showed no obvious toxicity.[30] We are therefore confident for further developments and that the colloids show promise for future application for therapeutic purposes.

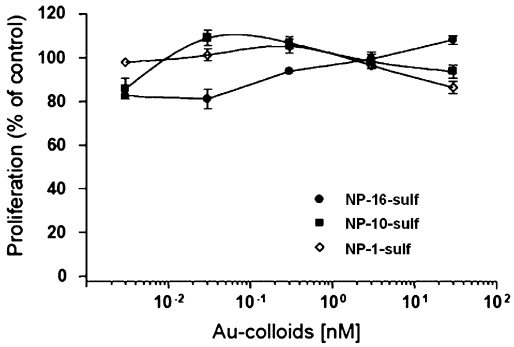

Fig. 5 Cell viability of Jurkat cells after incubation with different sulfated functionalized colloids.

Conclusions

Several series of sulfated cyclic and acyclic amino alcohols presented at gold colloids of different size were prepared and evaluated as multivalent selectin binding agents. All sulfated colloids showed very low IC_{50} values in the subnanomolar range for binding to P- and L-selectin. It was found that the chain length of the protective shell and the presence or absence of an amide bond in the spacer molecules considerably affect the binding properties of the particles. Binding to P-selectin is improved in the absence of an amide bond and for longer alkyl chains in the shell.

When compared to acyclic sulfated epitopes which do not differentiate between P-selectin and L-selectin, sulfated cyclic carbohydrate mimetics showed a clear selectivity for either P- or L-selectin. Preferential binding to P-selectin was always found when a *trans-trans* arrangement of the amino group at C4 of the aminopyran and the sulfate substituents at C2 and C3 was present. Accordingly, a moderate selectivity for P-selectin was found for the aminofuran with *trans-trans* configuration of the amino group and the substituents at C1 and C2.

For the series of colloids with acyclic epitopes the best binding properties were found for the disulfated serinol independent of the particle size. Here, an optimum in the interplay of surface charge and ligand flexibility seems to exist.

Functionalized gold colloids with multivalently presented sulfated polyol epitopes show excellent selectin binding properties and no signs of cytotoxicity. In addition, they are a valuable conceptional example for a significant improvement of ligand–receptor interactions when the ligand is presented in a multivalent fashion.

Experimental section

All reactions in aqueous solution were conducted in purified Millipore water. Organic solvents were distilled before use with the colloids. All other chemicals were purchased from commercial sources and used as received.

Aminopyran derivatives and aminofuran derivatives were prepared as described earlier: **1** and **2**,[21] **3** and **4**,[26] **5** and **6**,[27] **7** and **8**.[28]

NMR spectra were recorded with a JEOL lambda 400 spectrometer, IR spectra were obtained on a Nicolet 5 SXC spectrometer in ATR mode. SPR measurements were performed on a BIACORE X instrument.

Because of the rigidity of the alkyl chains in the thiol shells and the resulting large differences in the relaxation times of different protons, no integrals are given for the proton NMR data of the colloids.

Synthesis of Au/dodecanethiol

An amount of 0.435 g (5.00 mmol) of *tert*-butylamin-borane complex was added to a solution of 0.247 g $Au(PPh_3)Cl$ (0.50 mmol) and 0.25 ml dodecanethiol (1.00 mmol) in 40 ml of benzene. The mixture was stirred at 55 °C for 1 h before cooling to room temperature. Then 40 ml of ethanol were added and the precipitant separated by centrifugation. The black solid powder was washed with ethanol at least three times, dried under vacuum, and resolved in 25 ml of chloroform.

Synthesis of Au/citrate

A solution of 34 mg (0.09 mmol) of $HAuCl_4 \cdot 3\ H_2O$ in 360 ml of water was heated to reflux for 20 min. Under vigorous stirring a solution of 187 mg (0.52 mmol) of sodium citrate in 1.8 ml of water was added quickly. The reaction mixture was held under reflux for 3 h. Then the solution was cooled to 0 °C in an ice bath and filtered (0.2 µm pore size). A clear violet solution with a particle concentration of 2.6 nM was obtained and stored at 0 °C.

Synthesis of Au/MUDHSE

An amount of 95 mg of *N*-hydroxysuccinimid-11-mercaptoundecanoate (MUDHSE) (0.60 mmol) was dissolved in anhydrous dimethylformamide (DMF) and 1 ml of a 3 µM solution of dodecanethiol-protected gold nanoparticles in chloroform was added dropwise to the stirring solution. After 15 min the main part of the chloroform was removed under reduced pressure and the solution was stirred at r.t. for another 24 h. The nanoparticle solution was dialysed against 400 ml DMF three times, dried under vacuum and resolved in 15 ml of anhydrous DMF.

Three representative synthetic procedures for the preparation of the sulfated colloids are presented here: amine immobilization and subsequent sulfation for **NP-1-sulf** with a cyclic epitope, amine immobilization and sulfation for **NP-9-sulf** with an acyclic epitope and direct ligands substitution with the sulfated thiol for **NP-17-sulf**. Synthetic procedures for all other functionalized colloids can be found in the Supporting Information.

Synthesis of gold nanoparticles bearing aminopyran 1 (NP-1)

A solution of 4.2 mg **1** (0.02 mmol) in anhydrous DMF was added to 5 ml of a 0.2 µM solution of MUDHSE protected gold nanoparticles in DMF. After 30 min of stirring at r.t. 20 µl of triethylamine (0.14 mmol) was added and the mixture stirred for another 24 h. The clear colloid solution was dialysed against 300 ml of DMF for three times, dried under vacuum and resolved in 5 ml of anhydrous DMF.

Sulfation of NP-1 (NP-1-sulf)

At 0 °C 15.3 mg $SO_3 \cdot$DMF complex (0.10 mmol), dissolved in 1 ml of anhydrous DMF, was slowly dropped to 10 ml of a 0.1 µM solution of **NP-1** in anhydrous DMF. After 24 h of stirring at r.t. the clear solution was dialysed against 300 ml of DMF for one time and 300 ml of triple-distilled water for three times. For storage the colloid solution was diluted to a 0.03 µM concentration of nanoparticles.

^{1}H NMR (D_2O, 400 MHz): δ = 1.30 (*bs*), 1.32 (*s*), 1.47 (*s*), 1.59 (*m*), 1.68 (*m*), 2.30 (*bt*), 2.39 (*q*), 2.76 (*bs*), 4.01 (*m*), 4.18 (*m*), 4.46 (*m*), 4.54 (*m*).

ATR-IR: ν = 3448 cm^{-1} (w, ν(N–H)), 3075 (w), 2923 and 2852 (s, ν(C–H)), 2484 (w), 1687 and 1647 (s, ν(C═O)), 1529 (s, δ(N–H)), 1467 and 1207 (s, R–O–SO_2–OR′), 1058 (s), 985 (s), 810 (s), 582 (s).

Synthesis of gold nanoparticles bearing ethanolamine 9 (NP-9)

A solution of 9 µl ethanolamine **9** (0.15 mmol) in anhydrous DMF was added to 5 ml of a 0.2 µM solution of MUDHSE-protected gold nanoparticles in DMF. After 30 min of stirring at r.t. 20 µl triethylamine (0.14 mmol) was added and the mixture stirred for another 24 h. The clear colloid solution was dialysed against 300 ml of DMF for three times, dried under vacuum and resolved in 5 ml of anhydrous DMF.

Sulfation of NP-9 (NP-9-sulf)

At 0 °C 300 mg $SO_3 \cdot$DMF-complex (1.96 mmol), dissolved in 1 ml of anhydrous DMF, was slowly dropped to 10 ml of a 0.1 µM solution of **NP-9** in anhydrous DMF. After 24 h of stirring at r.t. the clear solution was dialysed against 300 ml of DMF for two times and 300 ml of triple-distilled water for three times. For storage the colloid solution was diluted to a 0.03 µM concentration of nanoparticles.

^{1}H NMR (D_2O, 400 MHz): δ = 1.25 (*bs*), 1.56 (*bs*), 2.22 (*bs*), 2.69 (*bs*), 3.45 (*bs*), 4.06 (*bs*).

ATR-IR: ν = 3302 cm^{-1} (s, ν(N–H)), 2918 and 2850 (s, ν(C–H)), 1686 and 1639 (s, ν(C═O)), 1532 (s, δ(N–H)), 1465–1452 and 1211 (s, R–O–SO_2–OR′), 1066 (s), 1020 (s), 959 (w), 719 (s), 579 (s).

Synthesis of 6-acetylsulfanylhexanoic acid

An amount of 1.50 g (7.67 mmol) of 6-bromohexanoic acid was dissolved in 15 ml of anhydrous DMF. A solution of 1.32 g (11.50 mmol) of potassium thioacetate in 15 ml of DMF was added dropwise and the mixture was stirred for 1 h. The solvent was removed under vacuum and water was added to the residue. Then the product was extracted with CH_2Cl_2 repeatedly. The organic

phases were collected and the solvent was removed under vacuum. The product was dried and 1.06 g (72% yield) of the product were obtained.

^{1}H NMR ($CDCl_3$, 400 MHz): δ = 1.35–1.45 (*m*, 2H), 1.57 (*quin*, 2H), 1.63 (*quin*, 2H), 2.30 (*s*, 3H) 2.33 (*t*, 2H), 2.85 (*t*, 2H).

Synthesis of *N*-hydroxysuccinimide-6-acetylsulfanylhexanoate

An amount of 1.06 g (5.58 mmol) of 6-acetylsulfanylhexanoic acid was added to a solution of 708 mg (6.16 mmol) of *N*-hydroxysuccinimide in 100 ml of CH_2Cl_2. A solution of 1.27 g (6.16 mmol) of dicyclohexylcarbodiimide (DCC) in 5 ml of CH_2Cl_2 was added dropwise and after a few minutes a white solid precipitated. The reaction mixture was stirred for 1 h. The solvent was removed under vacuum and the crude product was dissolved in little CH_2Cl_2 and filtered. The solvent was evaporated and 1.55 g of a brownish oil were obtained (98% yield).

^{1}H NMR ($CDCl_3$, 400 MHz): δ = 1.46 (*m*, 2H), 1.61 (*quin*, 2H), 1.74 (*quin*, 2H), 2.30 (*s*, 3H), 2.59 (*t*, 2H), 2.82 (*s*, 4H), 2.86 (*t*, 2H).

Synthesis of [5-(2-hydroxy-1-hydroxymethyl-ethylcarbamoyl)-pentyl]-*S*-thioacetate

An amount of 765 mg (8.41 mmol) of serinol **10** was added to 20 ml of a solution of 1.62 g (5.64 mmol) of *N*-hydroxysuccinimide-6-acetylsulfanylhexanoate in DMF. After a few minutes the solution became cloudy and the mixture was stirred for 30 min. The solvent was removed under vacuum and the residue was suspended in 50 ml of water. The suspension was stored over night at 4–8 °C. The white precipitate was filtered off, washed with water, dried under high vacuum and purified by chromatography (CH_2Cl_2). A white solid was obtained (448 mg, 30% yield).

^{1}H NMR ($CDCl_3$, 400 MHz): δ = 1.34 (*quin*, 2H), 1.55 (*quin*, 2H), 1.62 (*quin*, 2H), 2.19 (*t*, 2H), 2.29 (*s*, 3H), 2.82 (*t*, 2H), 3.72 (*ddd*, 4H), 3.92 (*quin*, 1H).

Synthesis of 17-sulf

[5-(2-Hydroxy-1-hydroxymethyl-ethyl-carbamoyl)pentyl]-*S*-thioacetate (52 mg, 0.20 mmol) was dissolved in 2 ml of DMF and 123 mg (0.80 mmol) of SO_3·DMF in 1 ml of DMF were added dropwise. The solution was stirred for 1 h. 3.2 ml of 1 M NaOH were added and the reaction mixture was stirred for 5 h. The completeness of the reaction was monitored by TLC. The product was not isolated but directly reacted with the Au/citrate nanoparticles.

Synthesis of NP-17-sulf

A solution of 0.20 mmol **17-sulf** in 6 ml of DMF/NaOH was added to 50 ml of a 2.6 nM aqueous solution of Au/citrate and the mixture was stirred for 72 h. Then the particles were dialysed against 600 ml of water for three times. After concentration of the solution to 10 ml a 12.7 nM solution of **NP-17-sulf** was obtained.

^{1}H NMR (D_2O, 400 MHz): δ = 1.37 (*m*), 1.59 (*m*), 1.66 (*m*), 2.26 (*t*), 2.71 (*m*), 4.09 (*m*), 4.38 (*m*).

SPR based competitive selectin-ligand binding assay[22]

Selectin-ligand binding was analyzed by surface plasmon resonance (SPR). First, the binding (detected as resonance units) of selectin-coated nanoparticles to a selectin ligand, immobilized on a sensor chip, was tested, and the resulting signal was henceforth referred to as 100% binding. Pre-incubation of the selectin-coated particles with varying concentrations of a selectin inhibitor (here a gold colloid with a ligand shell) decreased the binding signal. The calculated IC_{50} values (half inhibitory concentration) is the molar concentration of the inhibitor needed to reduce the binding signal to 50% of the initial value. Further details regarding the binding assay can be found in the ESI† and in Ref. 22.

Cytotoxicity assay

The Promega CellTiter 96® AQueous Cell Proliferation Assay was applied. L-selectin expressing T-cells (Jurkat) cells were seeded in 96-well plated at a density of 5000 cells/well. The Au-colloids **NP-1-sulf**, **NP-10-sulf** and **NP-16-sulf** were added at concentrations of 0.003 nM, 0.03 nM, 0.3 nM, 3 nM and 30 nM. In comparison to the untreated control cell proliferation was detected after 3 days incubation by measuring the conversion of the tetrazolium compound 3-(4,5-dimethylthiazol-2-yl)-5-(3-carboxymethoxyphenyl)-2-(4-sulfophenyl)-2*H*-tetrazolium (MTS) and an electron coupling reagent, phenazine ethosulfat (PES) into a water-soluble formazan that absorbs light at 490 nm by cellular dehydrogenases. The assay was performed in triplicates at each concentration. The untreated control was set to 100% proliferation.

Acknowledgements

The authors gratefully acknowledge financial support from the Deutsche Forschungsgemeinschaft within the Sonderforschungsbereich 765, the Fonds der Chemischen Industrie (PhD fellowship for F. P.) and the Alexander von Humboldt Foundation (Fellowship for S. Y.).

Notes and References

1 M. P. Bevilacqua and R. M. Nelson, *J. Clin. Invest.*, 1993, **91**, 379.
2 D. Vestweber and J. E. Blanks, *Physiol. Rev.*, 1999, **79**, 181.
3 K. Ley, D. C. Bullard, M. L. Arbones, R. Bosse, D. Vestweber, T. F. Tedder and A. L. Beaudet, *J. Exp. Med.*, 1995, **181**, 669.
4 W. S. Somers, J. Tang, G. D. Shaw and R. T. Camphausen, *Cell*, 2000, **103**, 467.
5 A. Leppänen, T. Yago, V. I. Otto, R. P. McEver and R. D. Cummings, *J. Biol. Chem.*, 2003, **278**, 26391.
6 F. Li, P. P. Wilkins, S. Crawley, J. Weinstein, R. D. Cummings and R. P. McEver, *J. Biol. Chem.*, 1996, **271**, 3255.
7 R. M. Nelson, O. Cecconi, W. G. Roberts, A. Aruffo, R. J. Linhardt and M. P. Bevilacqua, *Blood*, 1993, **82**, 3253.
8 A. Koenig, K. Norgard-Sumnicht, R. Linhardt and A. Varki, *J. Clin. Invest.*, 1998, **101**, 877.
9 M. Mammen, S.-K. Choi and G. M. Whitesides, *Angew. Chem.*, 1998, **110**, 2908, *Angew. Chem.*, Int. Ed., 1998, **37**, 2754.
10 M.-C. Bowman, T. E. Ballard, C. J. Ackerson, T. N. Tran, D. L. Feldheim, D. M. Margolis and C. Melander, *J. Am. Chem. Soc.*, 2008, **130**, 6896.
11 D. A. Giljohann, D. S. Seferos, W. L. Daniel, M. D. Massich, P. C. Patel and C. A. Mirkin, *Angew. Chem.*, 2010, **122**, 3352, *Angew. Chem. Int. Ed.*, 2010, **49**, 3280.
12 (*a*) M. De, P. S. Ghosh and V. M. Rotello, *Adv. Mater.*, 2008, **20**, 4225; (*b*) C. Kim, S. S. Agasti, Z. Zhu, L. Isaacs and V. M. Rotello, *Nat. Chem.*, 2010, **2**, 962.
13 C. M. Niemeyer, *Angew. Chem.*, 2001, **113**, 4254, *Angew. Chem., Int. Ed.*, 2001, **40**, 4128.
14 K. Riehemann, S. W. Schneider, T. A. Luger, B. Godin, M. Ferrari and H. Fuchs, *Angew. Chem.*, 2009, **121**, 886, *Angew. Chem., Int. Ed.*, 2009, **48**, 872.

15 I. Papp, J. Dernedde, S. Enders and R. Haag, *Chem. Commun.*, 2008, 5851.
16 J. Dernedde, A. Rausch, M. Weinhart, S. Enders, R. Tauber, K. Licha, M. Schirner, U. Zügel, A. von Bonin and R. Haag, *Proc. Natl. Acad. Sci. U. S. A.*, 2010, **107**, 19679.
17 Recent reviews on carbohydrate mimetics: (*a*) F. Pfrengle and H.-U. Reissig, *Chem. Soc. Rev.*, 2010, **39**, 549; (*b*) D. C. Koester, A. Holkenbrink and D. B. Werz, *Synthesis*, 2010, 3217.
18 Preliminary communication on the concept of selectin binding of these structures: J. Dernedde, S. Enders, H.-U. Reissig, M. Roskamp, S. Schlecht and S. Yekta, *Chem. Commun.*, 2009, 932.
19 N. Zheng, J. Fan and G. D. Stucky, *J. Am. Chem. Soc.*, 2006, **128**, 6550.
20 F. Porta, G. Speranza, Z. Krpetic, V. Dal Santo, P. Francescato and G. Scari, *Mater. Sci. Eng., B*, 2007, **140**, 187.
21 A. Al-Harrasi, F. Pfrengle, V. Prisyazhnyuk, S. Yekta, P. Koóš and H.-U. Reissig, *Chem.–Eur. J.*, 2009, **15**, 11632.
22 S. Enders, G. Bernhard, A. Zakrzewicz and R. Tauber, *Biochem. Biophys. Acta*, 2007, **1770**, 1441.
23 M. Daniel and D. Astruc, *Chem. Rev.*, 2004, **104**, 293.
24 K. B. Cederquist and C. D. Keating, *ACS Nano*, 2009, **3**, 256.
25 A. G. Klopocki, T. Yago, P. Mehta, J. Yang, T. Wu, A. Leppänen, N. V. Bovin, R. D. Cummings, C. Zhu and R. P. McEver, *J. Biol. Chem.*, 2008, **283**, 11493.
26 F. Pfrengle and H.-U. Reissig, *Chem.–Eur. J.*, 2010, **16**, 11915.
27 F. Pfrengle and H.-U. Reissig, *Beilstein J. Org. Chem.*, 2010, **6** (No. 75).
28 V. Dekaris, B. Bressel and H.-U. Reissig, *Synlett*, 2010, 47.
29 B. Fadeel and A. E. Garcia-Bennett, *Adv. Drug Delivery Rev.*, 2010, **62**, 362.
30 C. Lasagna-Reeves, D. Gonzales-Romero, M. A. Barria, I. Olmedo, A. Clos, V. M. Sadagopa Ramanujam, A. Urajama, L. Vergara, M. J. Kogan and C. Soto, *Biochem. Biophys. Res. Commun.*, 2010, **393**, 649.

